17. Fülöp, V., Moir, J. W. B., Ferguson, S. J. & Hajdu, J. Crystallisation and preliminary crystallographic study of cytochrome cd_1 nitrite reductase from *Thiosphaera pantotropha*. *J. Mol. Biol.* **232,** 1211–1212 (1993).
18. Berger, H. & Wharton, D. C. Small angle X-ray scattering studies of oxidised and reduced cytochrome oxidase from *Pseudomonas aeruginosa*. *Biochim. Biophys. Acta* **622,** 355–359 (1980).
19. Moore, G. R. & Pettigrew, G. W. *Cytochromes c: Evolutionary, Structural and Physicochemical Aspects* (Springer, Berlin, 1990).
20. Pettigrew, G. W. & Moore, G. R. *Cytochromes c: Biological Aspects* (Springer, Berlin, 1987).
21. Harutunyan, E. H. *et al.* The binding of carbon monoxide and nitric oxide to leghaemoglobin in comparison with other haemoglobins. *J. Mol. Biol.* **264,** 152–161 (1996).
22. Edwards, S. L., Kraut, J. & Poulos, T. L. Crystal structure of nitric oxide inhibited cytochrome-c peroxidase. *Biochemistry* **27,** 8074–8081 (1988).
23. Adman, E. T., Godden, J. W. & Turley, S. The structure of copper nitrite reductase from *Achromobacter cycloclastes* at five pH values, with NO_2^- bound and with type II copper depleted. *J. Biol. Chem.* **270,** 27458–27474 (1995).
24. Williams, P. A. thesis, Oxford Univ. (1996).
25. Poulos, T. L. Ligands and electrons and haem proteins. *Nature Struct. Biol.* **3,** 401–403 (1996).
26. Wittung, P. & Malmstrom, B. G. Redox-linked conformational changes in cytochrome *c* oxidase. *FEBS Lett.* **388,** 47–49 (1996).
27. Pascher, T., Chesick, J. P., Winkler, J. R. & Gray, H. B. Protein folding triggered by electron transfer. *Science* **271,** 1558–1560 (1996).
28. Kraulis, P. J. MOLSCRIPT: a program to produce both detailed and schematic plots of protein. *J. Appl. Crystallogr.* **24,** 946–950 (1991).
29. Merritt, E. A. & Murphy, M. E. P. Raster3D Version 2.0. A program for photorealistic molecular graphics. *Acta Crystallogr. D* **50,** 869–873 (1994).
30. Brünger, A. T. The free *R* value: a novel statistical quantity for assessing the accuracy of crystal structures. *Nature* **355,** 472–474 (1992).

Acknowledgements. We thank the ESRF and SRS Daresbury for data collection facilities; the EMBL outstation, Grenoble, for use of an image plate detector; M.L.D. Page for expert advice; R. Bryan and R. Esnouf for computing; K. Harlos for help with in-house data collection; F. Armstrong and J. Hirst for providing electrochemically reduced methyl viologen. This work was supported by MRC, BBSRC and EU-BIOTECH. The Oxford Centre for Molecular Sciences is funded jointly by BBSRC, EPSRC and MRC. N.F.W.S. was supported by a Wellcome Trust prize studentship. V.F. is a Royal Society university research fellow.

Correspondence and requests for materials should be addressed to P.A.W. (e-mail: pamela@scripps.edu), V.F. (e-mail: vilmos@biop.ox.ac.uk) or J.H. (e-mail: janos@xray.bmc.uu.se).

errata

The yeast genome directory

Nature **387** (suppl.) (1997)

In the list of authors given on page 5 of this supplement, the names of some authors were omitted or misspelled (asterisks). These were: R. Altmann; W. Arnold*; M. de Haan*; K. Hamberg; K. Hinni; L. Jones; W. Kramer; H. Küster*; K. C. T. Maurer*; D. Niblett; N. Paricio*; A. G. Parle-McDermott*; C. Rebischung; C. Richards; L. Rifkin*; J. Robben; C. Rodrigues-Pousada*; I. Schaaff-Gerstenschläger*; P. H. M. Smits*; Y. Su*; Q. J. M. van der Aart*; J. C. van Vliet-Reedijk*; A. Wach; M. Yamazaki*. □

Measurements of elastic anisotropy due to solidification texturing and the implications for the Earth's inner core

Michael I. Bergman

Nature **389,** 60–63 (1997)

Owing to a typographical error, this Letter appeared under the title "Measurements of electric anisotropy due to solidification texturing and the implications for the Earth's inner core". The word 'elastic' in the first line was erroneously replaced with 'electric'. □

cAMP-induced switching in turning direction of nerve growth cones

Hong-jun Song, Guo-li Ming & Mu-ming Poo

Nature **388,** 275–279 (1997)

The order of panels in Fig. 3 of this Letter is incorrect as published. Figure 3a–e should be labelled as f–j, and Fig. 3f–j should be labelled a–e. □

corrections

Synthesis and X-ray structure of dumb-bell-shaped C_{120}

Guan-Wu Wang, Koichi Komatsu, Yasujiro Murata & Motoo Shiro

Nature **387,** 583–586 (1997)

In this Letter, we overlooked a citation of G. Oszlanyi *et al.*, *Phys. Rev. B* **54,** 11849 (1996), who reported the observation of covalently bound $(C_{60})_2^{2-}$ dianions from the X-ray powder diffraction patterns of the metastable phases of KC_{60} and RbC_{60}. □

The complete genome sequence of the gastric pathogen *Helicobacter pylori*

Jean-F. Tomb, Owen White, Anthony R. Kerlavage, Rebecca A. Clayton, Granger G. Sutton, Robert D. Fleischmann, Karen A. Ketchum, Hans Peter Klenk, Steven Gill, Brian A. Dougherty, Karen Nelson, John Quackenbush, Lixin Zhou, Ewen F. Kirkness, Scott Peterson, Brendan Loftus, Delwood Richardson, Robert Dodson, Hanif G. Khalak, Anna Glodek, Keith McKenney, Lisa M. Fitzegerald, Norman Lee, Mark D. Adams, Erin K. Hickey, Douglas E. Berg, Jeanine D. Gocayne, Teresa R. Utterback, Jeremy D. Peterson, Jenny M. Kelley, Matthew D. Cotton, Janice M. Weidman, Claire Fujii, Cheryl Bowman, Larry Watthey, Erik Wallin, William S. Hayes, Mark Borodovsky, Peter D. Karp, Hamilton O. Smith, Claire M. Fraser & J. Craig Venter

Nature **388,** 539–547 (1997)

In this Article, we incorrectly stated that the amino acids lysine and arginine are twice as abundant in *H. pylori* proteins as they are in those of *Haemophilus influenzae* and *Escherichia coli*. This statement was derived from amino-acid analyses that compared absolute differences in abundance, but these do not reflect the frequencies with which amino acids are found in the organisms in question. The actual abundance of arginine in *H. pylori*, *H. influenzae* and *E. coli* is 3.5, 4.5 and 5.5%, respectively; the abundance of lysine in these organisms is 8.9, 6.3 and 4.4%, respectively. This oversight is particularly unfortunate because Russell H. Doolittle, who wrote an accompanying News and Views on our Article and brought this to our attention, was led to comment on the significance of our inaccurate observation. We regret this and any other misunderstanding that our error may have caused. □

Nature © Macmillan Publishers Ltd 1997

Nature © Macmillan Publishers Ltd 1997

months old) F-344 rats were first tested on the Morris swim task (six trials per day for four days), which requires that the rat learns the location of a submerged escape platform in a pool of water, on the basis of external landmarks. The performance measure, corrected integrated path length (CIPL)[25], is the sum of the distances from the target minus the shortest possible sum if the rat had swum directly to the platform at its mean speed. As reported previously[25], the old rats were impaired on this task (mean CIPL ± s.e.m. on day 4: young, 1.81 ± 0.61 m; old, 2.76 ± 0.39 m; $F_{1,10} = 4.99$, $P < 0.05$), but they were unimpaired when the platform was not submerged and a distinct visual cue was suspended above it (on final trial: young, 0.15 ± 0.07 m; old, 0.16 ± 0.10 m; $F_{1,10} = 0.90$, $P > 0.36$). Thus the old rats were deficient in spatial memory, a characteristic of hippocampal dysfunction, but exhibited normal visual association memory, which does not depend on an intact hippocampus[29].

Neurophysiological recording. The rats subsequently underwent the surgical implantation of a micromanipulator array that carried 12 tetrode recording probes, for parallel recording of groups of hippocampal neurons[1,21]. The rats were trained using a food reward to traverse a track 6 cm wide in the shape of a rectangular figure 8 (Fig. 1a), located in a moderately illuminated room with prominent visual landmarks and numerous tactile, auditory and olfactory spatial cues. Initially, the rats were confined to the north half of the apparatus by a removable partition that prevented access to or view of the other portion. The rats thus ran repeatedly (15–20 laps per episode) around a rectangular course. Three different manipulations were carried out to investigate the consistency of place-field maps on repeated visits to a fixed environment. The first was to allow the rats to spend ~25 min exploring the unfamiliar (south) portion of the track before returning to the familiar portion. This was carried out twice for each rat. In subsequent manipulations, rats were removed from the recording room for 1 h. In half of these sessions, they were returned to their home room; in the other half, they were allowed free exploration in each of six different rooms, for 10 min each, before returning to the recording apparatus. For five young and four old rats, the recording apparatus for the latter manipulations consisted of the north half of the figure 8. For two old rats and one young rat, the full apparatus (with no partition) was used as the test environment, instead of just the north half. (The details of the behavioural experience sequences are available as Supplementary Information.)

Each recording session thus consisted of 5 phases. Sleep 1, a period of ~30 min as the rat sat quietly and/or slept in a small 'nest'; Maze 1, in which the rat made multiple traversals of the track, always running in the same direction; Treatment, in which the rat was either transferred to the novel portion of the track or was removed from the room; Maze 2, in which the rat was returned to the track in its Maze 1 configuration; and Sleep 2, in which the rat was returned to the 'nest'. For four young–old rat pairs, data were available for two sessions in each of the three recording conditions. For technical and logistical reasons, the number of usable data sets was reduced for two rat pairs (Fig. 2).

Received 10 December 1996; accepted 25 April 1997.

1. Wilson, M. A. & McNaughton, B. L. Dynamics of the hippocampal ensemble code for space. *Science* **261,** 1055–1058 (1993).
2. O'Keefe, J. & Dostrovsky, J. The hippocampus as a spatial map. Preliminary evidence from unit activty in the freely-moving rat. *Brain Res.* **34,** 171–175 (1971).
3. Thompson, L. T. & Best, P. J. Long-term stability of place-field activity of single units recorded from the dorsal hippocampus of freely behaving rats. *Brain Res.* **509,** 299–308 (1990).
4. O'Keefe, J. & Nadel, L. *The Hippocampus as a Cognitive Map* (Clarendon, Oxford, 1978).
5. Uttl, B. & Graf, P. Episodic spatial memory in adulthood. *Psychol. Aging* **8,** 257 (1993).
6. Rapp, P. R. *et al.* Spatial learning and memory in freely moving monkeys. *Soc. Neurosci. Abstr.* **21,** 1710 (1995).
7. Barnes, C. A. Memory deficits associated with senescence: A neurophysiological and behavioral study in the rat. *J. Comp. Physiol. Psychol.* **931,** 74–104 (1979).
8. Barnes, C. A. Normal aging: Regionally specific changes in hippocampal synaptic transmission. *Trends Neurosci.* **17,** 13–18 (1994).
9. Geinisman, Y. *et al.* Hippocampal markers of age-related memory dysfunction: behavioral, electrophysiological and morphological perspectives. *Prog. Neurobiol.* **45,** 223–252 (1995).
10. Landfield, P. W. Hippocampal neurobiological mechanisms of age-related memory dysfunction. *Neurobiol. Aging* **9,** 571–579 (1988).
11. deToledo-Morrell, L. *et al.* Age-dependent alterations in hippocampal synaptic plasticity: relation to memory disorders. *Neurobiol. Aging* **9,** 581–590 (1988).
12. Markus, E. J. *et al.* Spatial information content and reliability of hippocampal CA1 neurons. *Hippocampus* **4,** 410–421 (1994).
13. Mizumori, S. J. Y., Lavoie, A. M. & Kalyani, A. Redistribution of spatial representation in the hippocampus of aged rats performing a spatial memory task. *Behav. Neurosci.* **110,** 1006 (1996).
14. Shen, J. thesis, Univ. Arizona (1996).
15. Quirk, G. J., Muller, R. U. & Kubie, J. L. The firing of hippocampal place cells in the dark depends on the rat's recent experience. *J. Neurosci.* **10,** 2008–2017 (1990).
16. McNaughton, B. L. *et al.* Deciphering the hippocampal polyglot: The hippocampus as a path integration system. *J. Exp. Biol.* **199,** 173–185 (1996).
17. McNaughton, B. L., Leonard, B. & Chen, L. Cortical-hippocampal interactions and cognitive mapping: A hypothesis based on reintegration of the parietal and inferotemporal pathways for visual processing. *Psychobiology* **17,** 230–235 (1989).
18. Muller, R. U., Kubie, J. L. & Saypoff, R. The hippocampus as a cognitive graph: Abridged version. *Hippocampus* **1,** 243–246 (1991).
19. Shapiro, M. L. & Hetherington, P. A. A simple network model simulates hippocampal place fields: parametric analyses and physiological predictions. *Behav. Neurosci.* **107,** 34–50 (1993).
20. Tsodyks, M. & Sejnowski, T. *Int. J. Neural Syst.* **6,** 81–86 (1995).
21. Gothard, K. M., Skaggs, W. E. & McNaughton, B. L. Dynamics of mismatch correction in the hippocampal ensemble code for space: Interaction between path integration and environmental cues. *J. Neurosci.* **16,** 8027–8042 (1996).
22. Knierim, J. J., Kudrimoti, H. S. & McNaughton, B. L. Place cells, head direction cells, and the learning of landmark stability. *J. Neurosci.* **15,** 1648–1659 (1995).
23. Skaggs, W. E. *et al.* in *Advances in Neural Information Processing Systems* Vol. 5 (eds Hanson, S. J., Cowan, J. D. & Giles, C. L.) 1030–1037 (Morgan Kaufmann, New York, 1993).
24. Samsonovich, A. thesis, Univ. Arizona (1997).
25. Gallagher, M., Burwell, R. & Burchinal, M. Severity of spatial learning impairment in aging: Development of a learning index for performance in the Morris water maze. *Behav. Neurosci.* **107,** 618–626 (1993).
26. Spencer, R. L., O'Steen, W. K. & McEwen, B. S. Water maze performance of aged Sprague-Dawley rats in relation to retinal morphologic measures. *Behav. Brain Res.* **68,** 139–150 (1995).
27. Barnes, C. A., McNaughton, B. L. & O'Keefe, J. Loss of place specificity in hippocampal complex-spike cells of senescent rat. *Neurobiol. Aging* **4,** 113–119 (1983).
28. Nadel, L., Willner, J. & Kurz, E. M. in *Context and Learning* (eds Tomie, P. D. B. & Tomie, A.) 385–406 (Earlbaum, Hillsdale, New Jersey, 1985).
29. Morris, R. G. M. *et al.* Place navigation impaired in rats with hippocampal lesions. *Nature* **297,** 681–683 (1982).
30. Kubie, J. L. & Ranck, J. B. Jr in *Neurobiology of the Hippocampus* (ed. Seifert, W.) 433–447 (Academic, London, 1983).

Supplementary information is available in *Nature*'s World-Wide Web site (http://www.nature.com) or as paper copy from Mary Sheehan at the London editorial office of *Nature*.

Acknowledgements. We thank R. D'Monte, J. L. Gerrard, W. E. Skaggs, K. Stengel, J. Wang and K. L. Weaver for assistance with data acquisition and analysis; P. J. Best, D. Chialvo, L. Nadel, W. E. Skaggs and F. A. Wilson for comments on the manuscript, and D. Clayman for instigating the NIA extramural program through which this work was supported. This work was supported by NIA and NIMH.

Correspondence and requests for materials should be addressed to C.A.B. (e-mail: carol@nsma.arizona.edu).

cAMP-induced switching in turning direction of nerve growth cones

Hong-jun Song, Guo-li Ming & Mu-ming Poo

Department of Biology, University of California at San Diego, La Jolla, California 92093-0357, USA

Development of the nervous system depends on the correct pathfinding and target recognition by the growing tip of an axon, the growth cone[1–3]. Diffusible or substrate-bound molecules present in the environment may serve as either attractants or repellents to influence the direction of growth-cone extension[4–11]. Here we report that differences in cyclic-AMP-dependent activity in a neuron may result in opposite turning of the growth cone in response to the same guidance cue. A gradient of brain-derived neurotrophic factor normally triggers an attractive turning response of the growth cone of *Xenopus* spinal neurons in culture, but the same gradient induces repulsive turning of these growth cones in the presence of a competitive analogue of cAMP or of a specific inhibitor of protein kinase A. This cAMP-dependent switch of the turning response was also found for turning induced by acetylcholine, but not for the turning induced by neurotrophin-3 (NT-3). Thus, in the presence of other factors that modulate neuronal cAMP-dependent activity, the same guidance cue may trigger opposite turning behaviours of the growth cone during its pathfinding in the nervous system.

Isolated spinal neurons in 14–20 h *Xenopus* cultures were used for these experiments. A microscopic gradient of brain-derived neurotrophic factor (BDNF) was created near the growth cone by pulsatile application of picolitres of BDNF-containing saline with a micropipette[12,13]. The tip of the micropipette was positioned

Nature © Macmillan Publishers Ltd 1997

100 μm from the centre of the growth cone and at a 45° angle with respect to the direction of neurite extension. The direction and total length of neurite extension were measured after 1 hour's growth in the presence of the gradient. The attractive turning response was revealed by a large percentage of growth cones turning towards the source of BDNF (Fig. 1a,b). Superimposed traces of the trajectory of growth cone extension for a population of neurons (Fig. 1c) and the scatter plot of the final position and total extension of growth cones (Fig. 1d) showed significant attractive turning of the growth cone in the BDNF gradient (50 μg ml^{-1} in the pipette). No significant turning response was observed when the pipette solution contained either a low concentration (0.5 μg ml^{-1}) of or no BDNF (Table 1). The attractive response to BDNF was apparently mediated by tyrosine-kinase receptors, because the effect was abolished by an inhibitor of tyrosine kinase K252a (200 nM; ref. 14). Table 1 summarizes the average turning angle and the

Table 1 Response of *Xenopus* nerve growth cones in chemical gradients

Chemicals in the pipette	Chemicals added in the bath†	$[Ca^{2+}]_o$ (mM)	Turning angle (degrees)‡	Net neurite extension (μm)‡	Turning responses (%)§ +	0	−	Number of cells examined
None	None	1	1.4 ± 2.3	16.7 ± 2.5	18	65	18	17
None	Rp-cAMPS	1	2.2 ± 3.8	11.6 ± 1.5	30	50	20	10
BDNF (50 μg ml^{-1})	None	1	14.3 ± 3.0**	19.6 ± 1.4	74	17	9	35
	K252a	1	− 1.0 ± 2.9	18.1 ± 2.4	25	42	33	12
	None	0.001	1.2 ± 4.5	24.5 ± 4.5*	24	47	29	17
	Rp-cAMPS	1	− 14.6 ± 3.7**	17.2 ± 2.2	6	24	70	17
	Rp-cAMPS	0.001	− 2.4 ± 6.4	19.2 ± 1.6**	18	55	27	11
	Sp-cAMPS	1	20.8 ± 5.2**	16.1 ± 1.4	91	9	0	11
	KT5720	1	− 18.4 ± 5.2**	22.5 ± 3.3	10	10	80	10
	ACPD	1	− 13.6 ± 2.9**	16.6 ± 2.3	0	20	80	10
BDNF (0.5 μg ml^{-1})	None	1	− 1.8 ± 4.3	16.1 ± 1.8	27	45	27	11
	Forsklin	1	13.3 ± 3.6**	23.2 ± 3.2	80	20	0	10
	1,9-dideoxy-forsklin	1	− 0.1 ± 3.4	18.3 ± 2.3	20	60	20	10
Forsklin (5 mM)	None	1	21.7 ± 4.2**	14.2 ± 1.6	80	20	0	10
	Rp-cAMPS	1	− 2.3 ± 4.1	13.7 ± 2.4	18	64	18	11
	None	0.001	18.0 ± 4.7**	36.5 ± 4.5**	80	20	0	10
1,9-Dideoxy-forsklin (5 mM)	None	1	2.5 ± 3.0	15.9 ± 2.9	30	50	20	10
NT-3 (50 μg ml^{-1})	None	1	9.4 ± 3.3*	16.0 ± 2.3	67	27	7	15
	None	0.001	14.6 ± 5.8*	27.6 ± 4.2*	73	13	13	15
	Rp-cAMPS	1	10.6 ± 4.4*	15.3 ± 4.7	60	33	7	15
ACh (100 mM)	None	1	13.5 ± 3.8**	14.5 ± 1.7	80	7	13	15
	Rp-cAMPS	1	− 9.6 ± 2.9*	14.7 ± 1.8	7	33	60	15

† K252a, 200 nM; Rp-cAMPS (adenosine 3′, 5′-cyclic phosphorothiolate-Rp), 20 μM; Sp-cAMPS (adenosine 3′, 5′-cyclic phosphorothiolate-Sp), 20 μM; KT5720, 200 nM; ACPD ((1*S*, 3*R*)-1-aminocyclopentane-1,3-dicarboxylic acid), 50 μM; forsklin (6β-[β′-(piperidino)propinyl]-forsklin), 5 μM; 1,9-dideoxy-forsklin, 5 μM. The drugs were added to the bath solution before the start of the chemical gradient and were present throughout the experiments.
‡ Values represent mean ± s.e.m. Values marked with * ($P < 0.05$) and ** ($P < 0.01$) were significantly different from the control (first two rows) using non-parametric Kruskal–Wallis test.
§ Growth cone turning responses were scored as follows: +, percentage of cells showing positive turning towards to the source of the chemical (turning angle > 5°); cells showing no turning (|turning angle| ≤ 5°); −, cells turning away (turning angle < −5°).

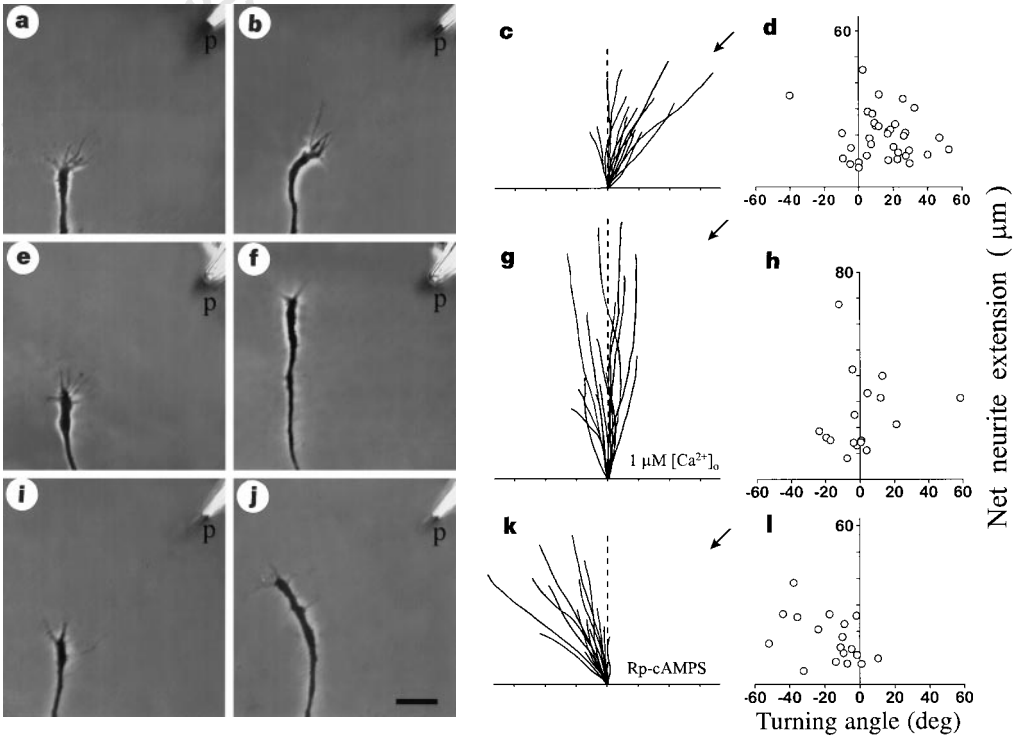

Figure 1 Attractive and repulsive turning of *Xenopus* growth cones induced by BDNF. A gradient of BDNF was applied in normal saline (**a**–**d**), in low-Ca^{2+} (1 μM) saline (**e**–**h**) and in saline containing 20 μM Rp-cAMPS (**i**–**l**). On the left are images of the growth cone at the onset (**a**, **e**, **i**) and at the end of the 1-h period (**b**, **f**, **j**). p: Tip of BDNF-containing pipette (50 μg ml^{-1} in the pipette). Scale bar, 20 μm. On the right are summary plots. Superimposed traces (**c**, **g**, **k**) depict the trajectory of neurite extension during the 1-h period for a sample population of 15 neurons. The origin is the centre of the growth cone at the onset, and the original direction of growth was vertical. Arrows indicate the direction of the gradient. Tick marks, 5 μm. Scatter plots (**d**, **h**, **l**) depict all data collected for each condition. Each point depicts the final angular position of a growth cone (abscissa) and its total neurite extension (ordinate) during the 1-h period.

Nature © Macmillan Publishers Ltd 1997

Nature © Macmillan Publishers Ltd 1997

percentage distribution of growth cones growing towards and away from the pipette.

To investigate the transduction mechanism underlying the turning response, we examined the roles of Ca^{2+} and cAMP, which both affect growth-cone behaviour[15,16]. First, extracellular Ca^{2+} ($[Ca^{2+}]_0$) was reduced from the normal level of 1 mM to 1 μM. Consistent with previous findings[13,17], this reduction in $[Ca^{2+}]_0$ led to an increased rate of neurite extension in these neurons. The attractive response was abolished (Fig. 1e–h and Table 1), however, indicating that an influx of Ca^{2+} may mediate the turning response induced by BDNF. The requirement for Ca^{2+} is similar for the potentiation of acetylcholine (ACh) release by BDNF at neuromuscular junctions in these cultures[18]. Second, the role of cAMP was examined: when a non-hydrolysable analogue competitor of cAMP, Rp-cAMPS[19], was added to the saline (at 20 μM), nearly all growth cones exhibited repulsive turning in the same BDNF gradient (Fig. 1i–l; Table 1). Bath addition of Rp-cAMPS (20 μM) in the absence of BDNF in the pipette solution had no effect on the direction of growth-cone extension (Table 1). Rp-cAMPS treatment apparently altered the action of endogenous cAMP in these neurons, because the same treatment also abolished the attractive turning response of these growth cones induced by a gradient of forskolin[12], a drug that activates adenyl cyclase and endogenous production of cAMP (Table 1). Addition of a specific inhibitor of protein kinase A(PKA), KT5720 (200 nM; ref. 14), to the bath also led to a repulsive turning in the BDNF gradient (Table 1), suggesting that the effect of Rp-cAMPS is probably due to its inhibition of PKA in these neurons[19]. Furthermore, bath application of Sp-cAMPS (20 μM; ref. 19), a cAMP analogue that activates PKA, resulted in a slight enhancement of the BDNF-induced attractive response (Fig. 2a; Table 1). Involvement of cAMP-dependent processes in BDNF-induced turning was also indicated by the following results. In the presence of 50 μM ACPD, a specific metabotropic glutamate receptor agonist that reduces the neuronal cAMP level[20], a BDNF gradient triggered clear repulsive responses (Fig. 2b; Table 1). A gradient of BDNF produced with a pipette containing 0.5 μg ml^{-1} BDNF, which was normally ineffective in attracting the growth cone, became highly attractive when forskolin was added to the bath (Fig. 2c,d; Table 1), whereas an inactive analogue, 1,9-dideoxy-forskolin, had no effect (Table 1). Finally, reduction of $[Ca^{2+}]_0$ to 1 μM completely abolished repulsive turning in the presence of Rp-cAMPS (Table 1), suggesting that both attractive and repulsive

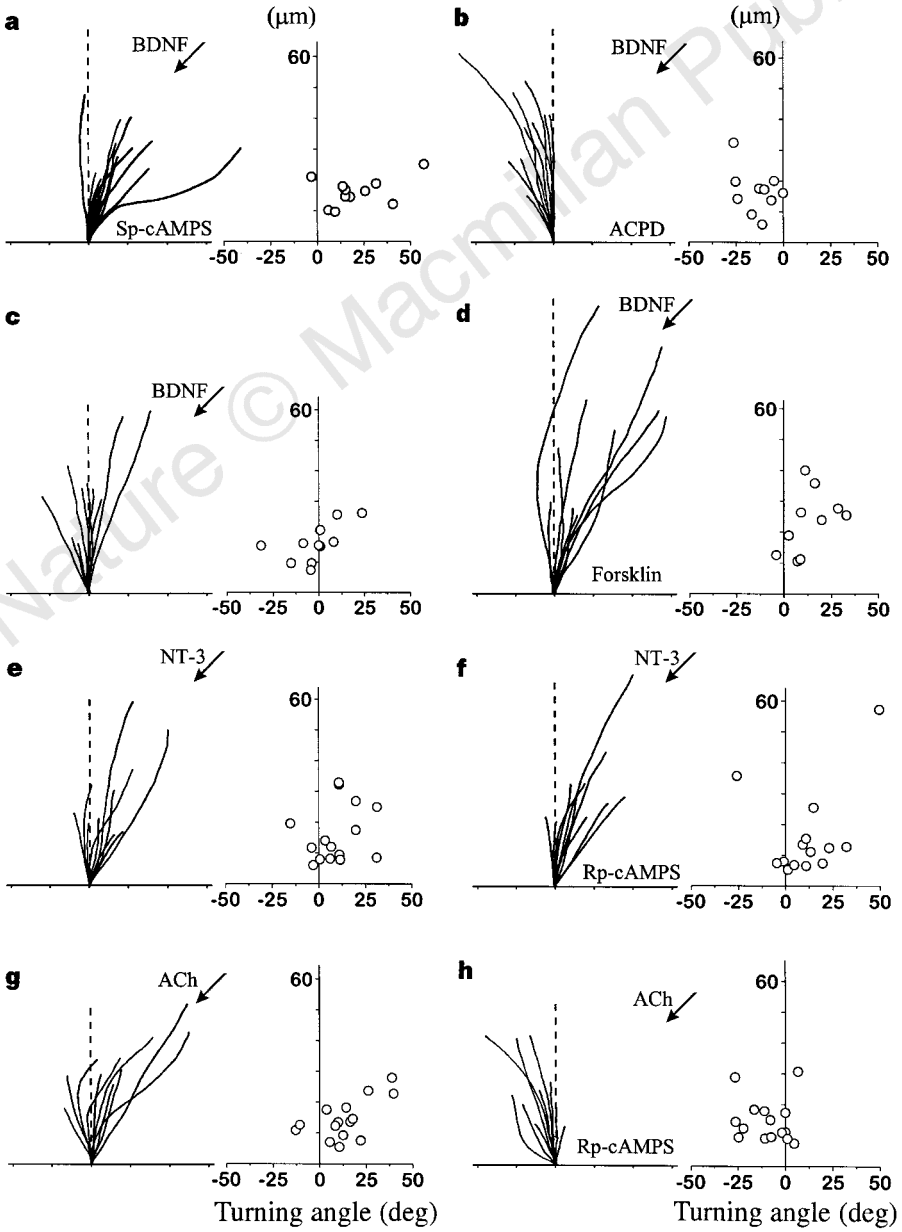

Figure 2 Growth cone turning under a variety of conditions. **a**, **b**, Turning responses induced by a BDNF gradient (50 μg ml^{-1} in the pipette) in a medium containing Sp-cAMPS (20 μM; **a**) and ACPD (50 μM; **b**). **c**, **d**, Turning responses induced by a gradient of BDNF (0.5 μg ml^{-1} in the pipette) in normal medium (**c**) and a medium containing 5 μM forskolin (**d**). **e**–**h**, Turning responses in the presence of a gradient of NT-3 and of ACh (50 μg ml^{-1} and 100 mM in the pipette), respectively, in normal medium (**e**, **g**) and in a medium containing Rp-cAMPS (20 μM; **f**, **h**).

Nature © Macmillan Publishers Ltd 1997

Nature © Macmillan Publishers Ltd 1997

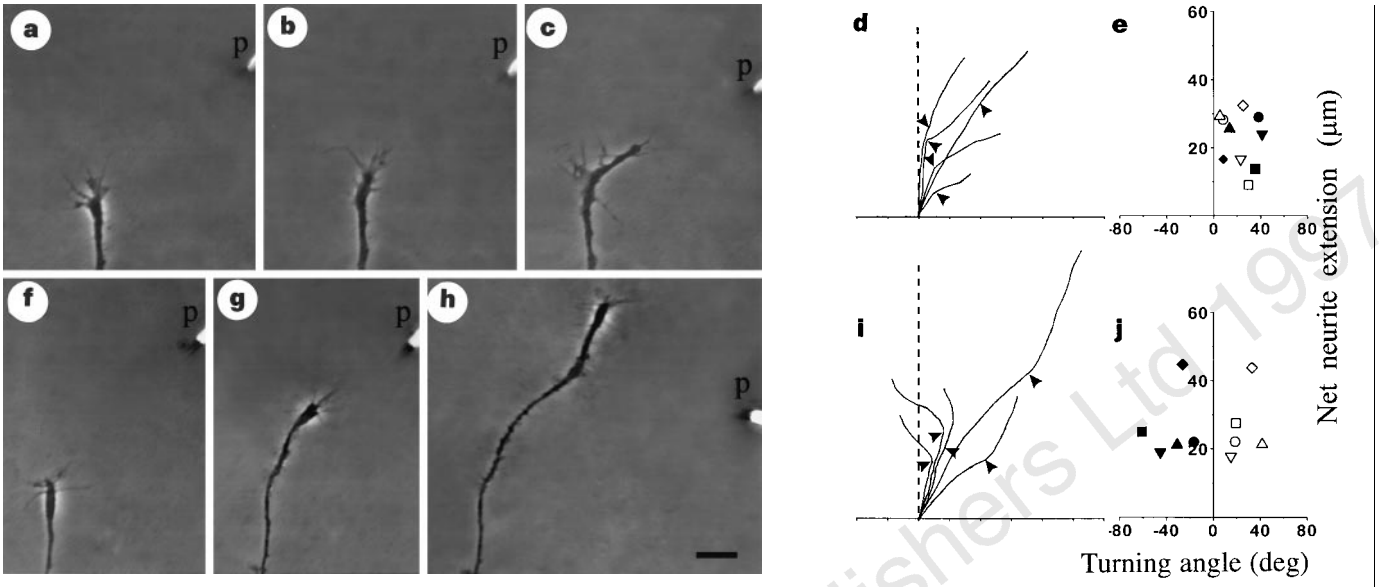

Figure 3 Switching from attractive to repulsive turning induced by KT5720. **a**–**c**, A neuron was exposed to the same BDNF gradient as for Fig. 1 for 1 h, followed by exposure to the same gradient for another hour with the pipette repositioned to a site 100 μm away and oriented 45° with respect to the new neurite direction, and KT7520 (200 nM) was added to the saline. **a**, At the onset; **b**, end of the first hour; **c**, end of the experiment. Tick marks, 10 μm. **d**, Superimposed traces of the trajectory of neurite extension in five neurons examined as that described in **a**–**c**. Triangles mark the end of the first hour. **e**, Scatter plot of the net neurite extension and final angular position of the growth cone at the end of the first (open symbols) and second hour (filled symbols). **f**–**j**, The same as that described in **a**–**e**, except that no drug was added into the saline during the second hour.

responses induced by BDNF require Ca^{2+} influx into the growth cone.

We also examined whether modulation of cAMP-dependent activity results in a switch between attractive and repulsive responses to the BDNF gradient in the same neuron. First we applied the standard BDNF gradient for 1 hour in normal saline, which induced attractive turning of the growth cone; the BDNF pipette was then repositioned 100 μm away and at a 45° angle with respect to the new direction of neurite extension for a further hour, either in the presence or absence of KT5720 (200 nM). As shown in Fig. 3a–e, there was a consistent switch to the repulsive response in the presence of KT5720, whereas there was further attractive turning in the absence of the drug (Fig. 3f–j). These results also indicate that the BDNF gradient did not desensitize the growth-cone response. The switch of the turning behaviour with KT5720 occurred without alteration in the rate of neurite growth (Fig. 3d,e) and both attractive and repulsive responses were preceded by asymmetric filopodia protrusion activity on two sides of the growth cone. No collapsing effect was observed after addition of KT5720.

The cultured *Xenopus* neurons also show attractive turning towards the source of neurotrophin-3 (NT-3), which acts through a different receptor (TrkC) from that used by BDNF (TrkB). Reduction of $[Ca^{2+}]_0$ to 1 μM, or addition of Rp-cAMPS (20 μM) was ineffective in altering the attractive resposne induced by NT-3 (Fig. 2e,f; Table 1). Thus the cAMP switch of the turning behaviour may operate only in neurons for specific types of guidance signals. The dependence of the effects of BDNF (but not of NT-3) on cAMP was also found for the long-term survival and growth of developing retinal ganglion cells in culture[21]. Gradients of ACh are known to be attractants for these *Xenopus* growth cones[13]: the transmitters appear to act by opening receptor channels to allow an influx of Ca^{2+} into the growth cone; the turning response is prevented by removing extracellular calcium[13]. Here we find Rp-cAMPS (20 μM) in the bath causes a repulsive turning of the growth cone in the presence of an ACh gradient (Fig. 2g,h; Table 1). The similar requirement for extracellular Ca^{2+} in ACh- and BDNF-induced turning responses, together with the findings that both ACh and BDNF can trigger an increase in cytosolic Ca^{2+} in these neurons[13,22], suggests that the cAMP switch may operate in the turning induced by Ca^{2+} influx. The concentration of calcium in the neuron can influence the production of cAMP in the neuron through activation of Ca^{2+}-dependent adenyl cyclase[23,24]. An extracellular gradient of BDNF or ACh may trigger a cytoplasmic Ca^{2+} gradient, which leads to a cAMP gradient within the growth cone and causes an attractive turning response[12]. On the other hand, elevation of cytosolic Ca^{2+} also inhibits growth-cone motility and neurite extension[15], so the cytosolic Ca^{2+} gradient by itself may induce a repulsive response in the growth cone; this effect is normally overridden by the attractive response owing to the cAMP gradient generated by the Ca^{2+} gradient. Inhibition of cAMP-dependent processes by Rp-cAMPS or KT5720, which block the attractive response, may thus reveal the repulsive effect of the cytosolic Ca^{2+} gradient. cAMP signalling presumably follows an increase in Ca^{2+} concentration, as a forskolin gradient can still induce an attractive response in a low-Ca^{2+} medium (Table 1).

A family of proteins known as netrins act as attractants for axons extending towards the ventral midline of the nervous system and as repellents for axons growing away from it[10,25–27]. Different netrin receptors may induce these different responses by modulating cAMP levels in the neuron. The action of transmitters and modulators is often mediated by regulation of second messengers[20,28–30] like cAMP. The presence or absence of these factors may thus switch the growth cone's response to the same guidance cue between attractive and repulsive. During its pathfinding in the developing embryo, a growth cone may be attracted to a 'guidepost' cell by a gradient of diffusible factor released by the cell. Upon arrival at the guidepost cell, changes in the cAMP level due to the presence of another signal, perhaps triggered by the contact of the guidepost cell, may switch the attractive response to a repulsive one, allowing the axon to grow away from the cell for its next stage of pathfinding. Finally, electrical activity can alter the level of cAMP in the active neuron through the activation of Ca^{2+}-dependent adenylyl cyclase[23,24] and also in nearby neurons through the action of neuromodulators released by the active neuron[30]. Activity-dependent

Nature © Macmillan Publishers Ltd 1997

Nature © Macmillan Publishers Ltd 1997

competition and refinement of nerve terminals near the target neuron may thus involve attraction or repulsion of the target-derived factor on the active and inactive nerve terminals, respectively, depending on their cAMP levels. □

Methods

Cell cultures. Cultures of *Xenopus* spinal neurons were prepared from the neural tube tissue of 1-day-old *Xenopus* embryos as described[12,13]. The tissue was dissociated in Ca^{2+}- and Mg^{2+}-free solution (115 mM NaCl, 2.5 mM KCl, 10 mM HEPES, 0.5 mM EDTA, pH 7.4) for 20 min and plated on the surface of clean glass coverslips. The culture was preincubated at room temperature (20–22 °C) for 14 h before use. The culture medium consisted of 49% (v/v) Leibovitz medium (GIBCO), 1% (v/v) fetal bovine serum (HyClone) and 50% (v/v) Ringer's solution (115 mM NaCl, 2 mM $CaCl_2$, 2.5 mM KCl, 10 mM HEPES, pH 7.4). The experiments were carried out in modified Ringer's solution (140 mM NaCl, 1 mM $MgCl_2$, 1 mM $CaCl_2$, 5 mM KCl, 10 mM HEPES, pH 7.4). Low-Ca^{2+} (1 μM) medium was modified Ringer's solution containing 0.9 mM $CaCl_2$, 4 mM EDTA.

Production of microscopic chemical gradients. Microscopic gradients of chemicals were produced as described[12,13]. Briefly, repetitive pressure injection of picolitre volumes of solutions containing the chemical was applied through a micropipette that had a tip opening of ~1 μm. The pressure was applied with an electrically gated pressure application system (Picospritzer General Valve). A standard pressure pulse of 3 p.s.i. in amplitude was applied for 20 ms to the pipette at a frequency of 2 Hz using a pulse generator (SD9, Grass Instruments). By measuring the size of droplet in the mineral oil after 50 pulses of repetitive ejection with the same pressure pulse parameters, the average volume of ejected solution per pulse was estimated to be ~1.5 pl. Analysis of the gradient[12,13] indicates that, under these pulse parameters, the average concentration of the chemical was $\sim 10^3$-fold lower than that in the pipette, and a concentration gradient of ~5–10% was created across a growth cone 10 μm wide, 100 μm away from the tip of the ejecting pipette. The total volume of the saline in the culture dish during the experiment was 5 ml. The final average bath concentration of BDNF at the end of the 1-h experiment was ~0.1 ng ml^{-1}.

Measurements of extension and turning of the growth cone. A phase-contrast inverted microscope (Nikon Diaphot) was used to observe the neurite growth. Microscopic images of the neurite were recorded with a CCD camera (Toshiba IK-541RA) attached to microscope and stored on videotape. To find the length of neurite extension, the entire trajectory of the neurite at the end of an hour was measured with a digitizer. To assay growth cone turning, the tip of the pipette containing the chemical was placed 100 μm away from the centre of the growth cone and at an angle of 45° with respect to the direction of initial direction of neurite extension. The direction of the neurite was determined by the last 10-μm segment of the neurite. The turning angle was defined by the angle between the original direction of neurite extension and a straight line connecting the positions of the growth cone at the onset and the end of the 1-h period. Only growth cones with a net extension >5 μm over the 1-h period were scored for the turning assay.

Received 30 December 1996; accepted 29 April 1997.

1. Bray, D. & Hollenbeck, P. J. Growth cone motility and guidance. *Annu. Rev. Cell Biol.* **4,** 43–61 (1988).
2. Keynes, R. & Cook, G. W. W. Axon guidance molecules. *Cell* **83,** 161–169 (1995).
3. Tessier-Lavigne, M. & Goodman, C. S. The molecular biology of axon guidance. *Science* **274,** 1123–1133 (1996).
4. Gundersen, R. W. & Barrett, J. N. Neuronal chemotaxis: chick dorsal root axons turn towards high concentrations of nerve growth factor. *Science* **206,** 1079–1080 (1979).
5. Bonhoeffer, F. & Huf, J. Recognition of cell types by axonal growth cones *in vitro*. *Nature* **288,** 162–164 (1980).
6. Lumsden, A. G. & Davies, A. M. Earliest sensory nerve fibres are guided to peripheral targets by attractants other than nerve growth factor. *Nature* **306,** 786–788 (1983).
7. Tessier-Lavigne, M., Placzek, M., Lumsden, A. G., Dodd, J. & Jessell, T. M. Chemotropic guidance of developing axons in the mammalian central nervous system. *Nature* **336,** 775–778 (1988).
8. Heffner, C. D., Lumsden, A. G. & O'Leary, D. D. Target control of collateral extension and directional axon growth in the mammalian brain. *Science* **247,** 217–220 (1990).
9. Pini, A. Chemorepulsion of axons in the developing mammalian central nervous system. *Science* **261,** 95–98 (1993).
10. Colamarino, S. A. & Tessier-Lavigne, M. The axonal chemoattractant netrin-1 is also a chemorepellent for trochlear motor axons. *Cell* **81,** 621–629 (1995).
11. Nakamoto, M. *et al.* Topographically specific effects of ELF-1 on retinal axon guidance *in vitro* and retinal axon mapping *in vivo*. *Cell* **86,** 755–766 (1996).
12. Lohof, A. M., Quillan, M., Dan, Y. & Poo, M.-m. Asymmetric modulation of cytosolic cAMP activity induces growth cone turning. *J. Neurosci.* **12,** 1253–1261 (1992).
13. Zheng, J. Q., Felder, M., Connor, J. A. & Poo, M.-m. Turning of nerve growth cones induced by neurotransmitters. *Nature* **368,** 140–144 (1994).
14. Kase, H. *et al.* K-252 compounds, novel and potent inhibitors of protein kinase C and cyclic nucleotide-dependent protein kinases. *Biochem. Biophys. Res. Commun.* **142,** 436–440 (1987).
15. Kater, S. K., Mattson, M. P., Cohan, C. & Conner, J. A. Calcium regulation of the neuronal growth cone. *Trends Neurosci.* **11,** 317–323 (1988).
16. Kim, Y.-t. & Wu, C. F. Reduced growth cone motility in cultured neurons from *Drosophila* memory mutants with a defective cAMP cascade. *J. Neurosci.* **16,** 5593–5602 (1996).
17. Bixby, J. L. & Spitzer, N. C. Early differentiation of vertebrate spinal neurons in the absence of voltage-dependent Ca^{2+} and Na^{+} influx. *Dev. Biol.* **106,** 89–96 (1984).
18. Lohof, A. M., Ip, N. Y. & Poo, M.-m. Potentiation of developing neuromuscular synapses by the neurotrophins NT-3 and BDNF. *Nature* **363,** 350–353 (1993).
19. Rothermel, J. D. & Parker Botelho, L. H. A mechanistic and kinetic analysis of the interactions of the diastereoisomers of adenosine 3′,5′-(cyclic)phosphorothioate with purified cyclic AMP-dependent protein kinase. *J. Biochem.* **251,** 757–762 (1988).
20. Pin, J.-p. & Duvoisin, R. The metabotropic glutamate receptors: structure and functions. *Neuropharmacology.* **34,** 1–26 (1995).
21. Meyer-Franke, A., Kaplan, M. R., Pfrieger, F. W. & Barres, B. A. Characterization of the signaling interactions that promote the survival and growth of developing retinal ganglion cells in culture. *Neuron* **15,** 805–819 (1995).
22. Stoop, R. & Poo, M.-m. Synaptic modulation by neurotrophic factors: differential and synergistic effects of brain-derived neurotrophic factor and ciliary neurotrophic factor. *J. Neurosci.* **16,** 3256–3264 (1996).
23. Wayman, G. A. *et al.* Synergistic activation of the type I adenylyl cyclase by Ca^{2+} and G_s-coupled receptors *in vivo*. *J. Biol. Chem.* **269,** 25400–25405 (1994).
24. Yovell, Y., Kandel, E. R., Dudai, Y. & Abrams, T. W. A quantitative study of the Ca^{2+}/calmodulin sensitivity of adenylyl cyclase in *Aplysia*, *Drosophila*, and rat. *J. Neurochem.* **59,** 1736–1744 (1992).
25. Hamelin, M., Zhou, Y., Su, M.-w., Scott, I. M. & Culotti, J. G. Expression of the UNC-5 guidance receptor in the touch neurons of *C. elegans* steers their axons dorsally. *Nature* **364,** 327–330 (1993).
26. Wadsworth, W. G., Bhatt, H. & Hedgecock, E. M. Neuroglia and pioneer neurons express UNC-6 to provide global and local netrin cues for guiding migrations in *C. elegans*. *Neuron* **16,** 35–46 (1996).
27. Mitchell, K. J. *et al.* Genetic analysis of netrin genes in *Drosophila*: Netrins guide CNS commissural axons and peripheral motor axons. *Neuron* **17,** 203–215 (1996).
28. Cooper, J. R., Bloom, F. E. & Roth, R. H. *The Biochemical Basis of Neuropharmacology* (7th edn, Oxford University Press, New York, 1996).
29. Laufer, R. & Changux, J. Calcitonin gene-related peptide elevates cyclic AMP levels in chick skeletal muscle: possible neurotrophic role for a coexisting neuronal messenger. *EMBO J.* **6,** 901–906 (1987).
30. Hempel, C. M., Vincent, P., Adams, S. R., Tsien, R. Y. & Selverston, A. I. Spatio-temporal dynamics of cyclic AMP signals in an intact neural circuit. *Nature* **384,** 166–169 (1996).

Acknowledgements. This work was supported by a grant from the NIH.

Correspondence and requests for materials should be addressed to M.-m.P. (e-mail: mpoo@ucsd.edu).

Synapse specificity of long-term potentiation breaks down at short distances

Florian Engert & Tobias Bonhoeffer

Max Planck Institute for Psychiatry, Am Klopferspitz 18A, 82152 München-Martinsried, Germany

Long-term potentiation (LTP), the long-lasting increase in synaptic transmission, has been proposed to be a cellular mechanism essential for learning and memory, neuronal development, and circuit reorganization. In the original theoretical[1] and experimental[2] work it was assumed that only synapses that had experienced concurrent pre- and postsynaptic activity are subject to synaptic modification. It has since been shown, however, that LTP is also expressed in synapses on neighbouring neurons that have not undergone the induction procedure[3–5]. Yet, it is still believed that this spread of LTP is limited to adjacent postsynaptic cells, and does not occur for synapses on neighbouring input fibres[2,6,7]. However, for technical reasons, tests for 'input specificity' were always done for synapses relatively far apart. Here we have used a new local superfusion technique, which allowed us to assess the synaptic specificity of LTP with a spatial resolution of ~30 μm. Our results indicate that there is no input specificity at a distance of less than 70 μm. Synapses in close proximity to a site of potentiation are also potentiated regardless of their own history of activation, whereas synapses far away show no potentiation.

Synaptic specificity of LTP was examined for synapses between the Schaffer collaterals and the CA1 region in organotypic slice cultures of rat hippocampus[3,8]. By using a local superfusion technique[9] we localized and individually activated neighbouring groups of synapses with a spatial resolution of less than 30 μm.

Nature © Macmillan Publishers Ltd 1997